Am J Physiol Cell Physiol 302: C1371–C1381, 2012.
First published February 8, 2012; doi:10.1152/ajpcell.00254.2011.

Impaired insulin-stimulated myosin phosphatase Rho-interacting protein signaling in diabetic Goto-Kakizaki vascular smooth muscle cells

Jin Hee Lee,[1,2] Thomas Palaia,[1] and Louis Ragolia[1,2]

[1]*Vascular Biology Institute, Winthrop-University Hospital, Mineola, New York; and* [2]*School of Medicine, Stony Brook University, Stony Brook, New York*

Submitted 19 July 2011; accepted in final form 3 February 2012

Lee JH, Palaia T, Ragolia L. Impaired insulin-stimulated myosin phosphatase Rho-interacting protein signaling in diabetic Goto-Kakizaki vascular smooth muscle cells. *Am J Physiol Cell Physiol* 302: C1371–C1381, 2012. First published February 8, 2012; doi:10.1152/ajpcell.00254.2011.—Insulin resistance associated with Type 2 diabetes contributes to impaired vasorelaxation and therefore contributes to the enhanced incidence of hypertension observed in diabetes. In this study, we examined the role of insulin on the association of the myosin-binding subunit of myosin phosphatase (MYPT1) to myosin phosphatase Rho-interacting protein (MRIP), a relatively novel member of the myosin phosphatase complex that directly binds RhoA in vascular smooth muscle cells (VSMCs). Through a series of molecular and cellular studies, we investigated whether insulin stimulates the binding of MRIP to MYPT1 and compared the results generated from VSMCs isolated from both Wistar-Kyoto (WKY) control and Goto-Kakizaki (GK) diabetic rats. We demonstrate for the first time that insulin stimulates the binding of MRIP to MYPT1 in a dose- and time-dependent manner, as determined by immunoprecipitation, implying a regulatory role for MRIP in insulin-induced vasodilation signaling via MYPT1 interaction. VSMCs from GK model of Type 2 diabetes had impaired insulin-induced MRIP/MYPT1 binding as well as reduced MRIP expression. Adenovirus-mediated overexpression of MRIP in GK VSMCs led to significantly improved insulin-stimulated MRIP/MYPT1 binding. Finally, insulin-stimulated MRIP translocation out of stress fibers, which was observed in control VSMCs, was impaired in GK VSMCs. We believe the impaired expression of MRIP, and therefore decreased insulin-stimulated MRIP/MYPT1 association, in the GK diabetic model may contribute to the impaired insulin-mediated vasodilation observed in the diabetic vasculature and provides a novel therapeutic strategy for the treatment of Type 2 diabetes.

insulin resistance; signaling pathways; myosin-binding subunit of myosin phosphatase

INCREASED CONTRACTILITY of vascular smooth muscle cells (VSMCs) in combination with defective vasorelaxation are the earliest abnormalities observed in atherosclerosis, diabetes, and hypertension (8, 15, 35). Insulin is a potent vasodilator involved in vascular smooth muscle contraction, migration, and growth in the normal vasculature. Insulin resistance, present in Type 2 diabetes, contributes to the enhanced atherosclerosis/restenosis associated with this condition (2, 17, 18). The exact mechanisms of insulin action related to VSMC relaxation are unknown. Therefore, studies designed to extend further our understanding of the molecular basis of insulin's effects on blood vessels and their interaction with inflammatory and vasoconstrictive agents under normal, hyperglycemic, and insulin resistant conditions are warranted.

Address for reprint requests and other correspondence: L. Ragolia, Vascular Biology Institute, Winthrop-Univ. Hospital, 222 Station Plaza North, Suite 505-B, Mineola NY 11501 (e-mail: LRagolia@Winthrop.org).

Smooth muscle contraction and relaxation is largely mediated by phosphorylation and dephosphorylation of myosin regulatory light chain (MLC20) by myosin light chain kinase (MLCK) and phosphatase (MLCP), respectively (11, 34). MLCP appears to be the critical phosphatase regulating smooth muscle contractility and is widely recognized to be the common target of signaling pathways that modulates smooth muscle tone. These include the RhoA/Rho kinase (19, 39), the endogenous MLCP inhibitor, CPI-17 (21), and the arachidonic acid pathway (13). The precise mechanisms of MLCP regulation are not fully understood.

MLCP holoenzyme consists of three subunits, the 38-kDa catalytic subunit of protein phosphatase-1, a large 110- to 130-kDa regulatory subunit (MYPT1), and a small 20-kDa subunit of unknown function (13, 29). MYPT1 binds to myosin and regulates the catalytic activity of the phosphatase (14, 16). Phosphorylation of MYPT1 by an associated kinase results in an inhibition of phosphatase activity (16). Studies have revealed that the active GTP-bound Rho was the small guanosine triphosphate that specifically interacts with MYPT1 (16). Rho-associated kinase directly phosphorylates MLC20 (23), CPI-17 (20), and MYPT1, and consequently inactivates MLCP, resulting in increased MLC20 phosphorylation and contraction of smooth muscle (16). The pathway leading from receptor to G proteins and then to the ultimate inhibition of the phosphatase is unknown.

Recent studies have shown that RhoA/Rho-kinase activity can influence the pathogenesis of vascular diseases, including hypertension, coronary artery spasm, and neointimal formation. Vasoconstrictors such as lysophosphatidic acid (LPA), thromboxane A_2, and angiotensin II (ANG II) inhibit MLCP via a RhoA/Rho-kinase-dependent mechanism. In contrast, our laboratory demonstrated that the insulin is a potent vasodilator of VSMCs through insulin receptor substrate-1 (IRS-1)→phosphatidylinositol 3-kinase (PI3-K)→inducible nitric oxide synthase (iNOS)→NO-cGMP and cGMP-dependent protein kinase 1α (cGKIα) signaling; insulin inhibits RhoA/Rho-associated kinase (ROK) activity by inducing an accumulation of cGMP and activating cGKIα, resulting in MLCP activation (5). Therefore, increases in MLCP activity by inhibition of the RhoA/Rho-kinase-mediated signaling pathway with insulin stimulation attenuate the contractile response (5, 33). RhoA proteins are primarily found as the GDP-bound (inactive) form in the cytosol fraction of unstimulated cells or tissues. When stimulated, the small G protein translocates from the cytosol to the membrane fraction as the GTP-bound (active) form. RhoA activates Rho-kinase, resulting in phosphorylation of MYPT1, and reduces MLCP activity. Rho-associated kinase-α (ROK-α), activated by the small GTPase, RhoA, phosphorylates MYPT1 at threonine 696, leading to the inactivation of MLCP

(10, 19) independent of intracellular calcium concentration (16). These signaling pathways can be antagonized by a vasodilator, insulin, resulting in MLCP activation and vasodilation (5, 26). In addition to RhoA/ROK-α (19), other downstream signaling pathways that inhibit MLCP activity have been discovered recently, including protein kinase C (PKC) activation of the inhibitory phosphoprotein CPI-17 (9) and arachidonic acid (13). Like PKC, ROK-α also phosphorylates CPI-17 at threonine 38 and thereby becomes a potent inhibitor of MLCP (38).

Recently, a new trafficking protein targeting MLCP to myosin has been found (36), which provides the direct interaction between RhoA/Rho-kinase and MLCP. Myosin phosphatase-Rho interacting protein (MRIP) binds to both RhoA and MYPT1 playing an important role in the regulation of MLC20 phosphorylation in response to vasoconstrictors(30). MRIP activates the MLCP activity of the holoenzyme but not the catalytic subunit alone, indicating that the activation is due to the binding of MRIP to the myosin phosphatase targeting subunit MYPT1. Interestingly, the activation of phosphatase was specific to myosin as substrate, and MRIP directly binds myosin, facilitating the myosin/MLCP interaction. MRIP silencing prevents LPA-mediated MYPT1 phosphorylation, and inhibition of MLCP activity. Silencing of MRIP also leads to loss of stress fiber-associated RhoA, suggesting that MRIP is a scaffolding protein linking RhoA to myosin phosphatase regulation (30). Another consequence of MRIP gene silencing is that basal and agonist-stimulated contractile responses are increased. Gene silencing of MRIP consistently and significantly increased myosin phosphorylation as well as stress fiber formation in cells. These data indicate that MRIP is an important regulatory component that controls the RhoA signaling pathway, and therefore regulates MLCP activity and myosin phosphorylation in cells (22). The regulation and intracellular targeting of the MLCP complex is, however, incompletely understood.

Our previous data indicate that aortic RhoA/Rho-kinase activity is increased in diabetic Goto-Kakizaki (GK) rats compared with that of the control Wistar-Kyoto (WKY) rat as determined by isometric tension measurement (26). Because Rho-kinase is upstream of MYPT1, increased phosphorylation of MYPT1 parallels Rho-kinase activity (10, 19). We hypothesized that impaired insulin-induced RhoA inhibition along with increased RhoA activity in GK VSMCs (10, 19) may be the result of either abnormal MRIP expression and/or regulation. In this study, we investigated the precise mechanisms responsible for insulin's control of RhoA-MRIP regulation of MLCP and determined how this pathway is dysregulated in GK VSMCs.

MATERIALS AND METHODS

Animal and tissue preparation. A colony of Type 2 diabetic GK rats was established at Winthrop University Hospital with animals originally supplied by Dr. Robert V. Farese (James A. Haley Veterans' Hospital, Tampa, FL) as detailed earlier (3, 25). WKY rats were purchased from Taconic Farms (Germantown, NY) and used as controls as in our previous publications (3, 25, 32). Both weight-matched WKY and GK rats were euthanized at the age of 8 wk with 95% CO_2 inhalation, which was approved by the Institutional Laboratory Animal Care and Use Committee of Winthrop University Hospital. The thoracic aorta of rats were rapidly and carefully excised and placed in ice-cold PBS. Endothelium removal was performed by gentle rotation around a thin polished metal stick as previously described (26, 28). Rings from denuded aortas were minced and homogenized with lysis buffer to yield the protein with Gentle MACS Dissociator, following the manufacturer's protocol (Macs Miltenyi Biotec).

Culture of VSMCs and treatment with insulin. VSMCs in primary culture were obtained by enzymatic digestion of the aortic media of male WKY and GK rats with body weights of 200–220 g, as described in our recent publications (4, 26). Procedures involving animals and their care were conducted in conformity with institutional guidelines in compliance with international laws and policies (National Institutes of Health *Guide for the Care and Use of Laboratory Animals*, National Research Council, 2010, 8th ed.). Unless otherwise indicated, primary cultures of VSMCs were maintained in α-MEM (Invitrogen) containing 10% FBS (Invitrogen) and 1% antibiotic-antimycotic mixture (Invitrogen). Subcultures of VSMCs at *passage 5* were used in all experiments and were grown for 9–10 days. Prior to each experiment, cells were serum starved for 24 h in serum-free α-MEM containing 1% antibiotics and 5.5 mM glucose. The next day,

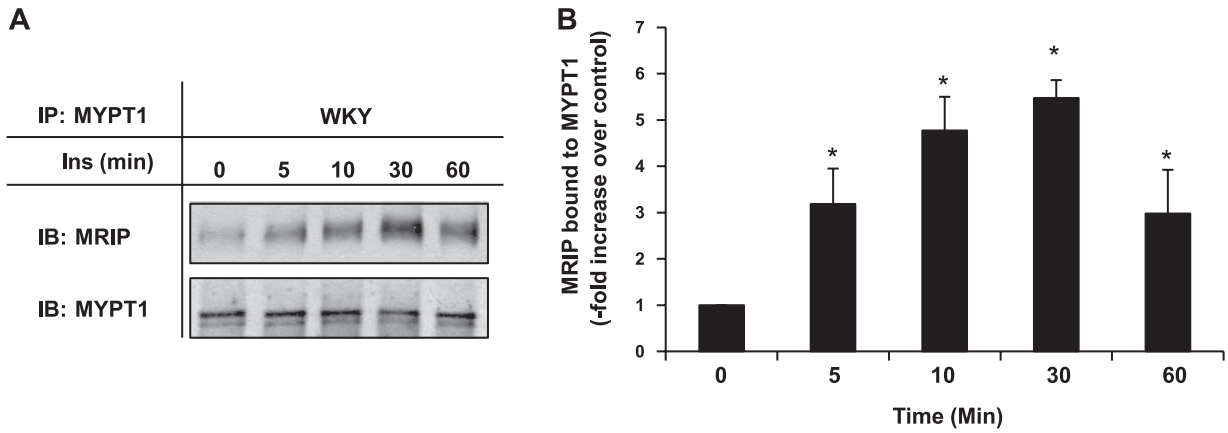

Fig. 1. Insulin increases the binding of myosin phosphatase Rho-interacting protein (MRIP) to myosin phosphatase targeting subunit 1 (MYPT1) in a time-dependent manner. Wistar-Kyoto (WKY) vascular smooth muscle cells (VSMCs) were exposed to insulin (Ins; 100 nM) for 0, 5, 10, 30, and 60 min. Equal amounts of protein cell lysates (500 μg) were resolved by SDS-PAGE after immunoprecipitation (IP) with MYPT1 as described in MATERIALS AND METHODS. *A*: MRIP and MYPT1 levels were measured by Western analysis. IB, immunoblot. *B*: protein intensity was quantitated by densitometric analysis and normalized to the abundance of MYPT1 ($n = 4$). *$P < 0.05$ vs. control.

cells were exposed to insulin (0–1,000 nM) for 10 min where indicated.

Transfection of VSMCs with small interfering RNA targeting MRIP. MRIP-specific oligonucleotides were predicted using Oligoengine and Dharmacon programs. A 21-bp oligonucleotide corresponding to bp 2037–2055 of the rat MRIP cDNA was synthesized by Dharmacon. Small interfering (si)control (siCon), which is nontargeting siRNA no. 1 from Dharmacon, was used to demonstrate the nonspecific effect of siRNA transfection. VSMCs were transfected with Amaxa Nucleofector (Lonza) by electroporation with siCon or siRNA targeting MRIP (siMRIP) following the manufacturer's instructions. Forty-eight hours after transfection, cells were serum starved for 24 h and experiments were performed as described above.

Overexpression of MRIP with adenovirus (Ad-MRIP-FLAG) treatment in VSMC. Adenovirus constructed with MRIP-FLAG fusion at the NH_2 terminus were made at the Gene Transfer Vector Core (University of Iowa, Iowa City) as described earlier (1). VSMCs were grown to 80% confluency and cells were washed with serum-free media then treated with Ad5CMV control or Ad-MRIP-FLAG for 4 h with agitation once per hour. After 4 h, serum was added to the cells and incubated overnight. The next day cells were washed with fresh media and cultured for an additional 24 h. Cells were serum starved for 24 h before the experiments with insulin.

Immunoprecipitation. Cells were lysed in a RIPA buffer (Thermo Scientific) containing 25 mM Tris·HCl (pH 7.6), 1 mM DTT, 250 mM NaCl, 0.1% SDS, 1% NP-40, and 1% deoxycholate, supplemented with a protease and phosphatase inhibitor cocktail (Thermo Scientific) containing 100 mM NaF, 50 mM sodium pyrophosphate, β-glycerophosphate, 20 μM sodium orthovanadate, 2 μM microcystin, 50 μM bestatin, 1 mM 4-(2-aminoethyl)benzenesulfonyl fluoride (AEBSF), 500 mM EDTA, 15 μM E64, 20 μM leupeptin, and 800 nM aprotinin. Lysates were centrifuged for 30 min at 14,000 *g*. Equal amounts (500 μg) of protein were immunoprecipitated with the anti-MYPT1 (Santa Cruz) using magnetic protein G beads (Invitrogen) and DynaMag-2

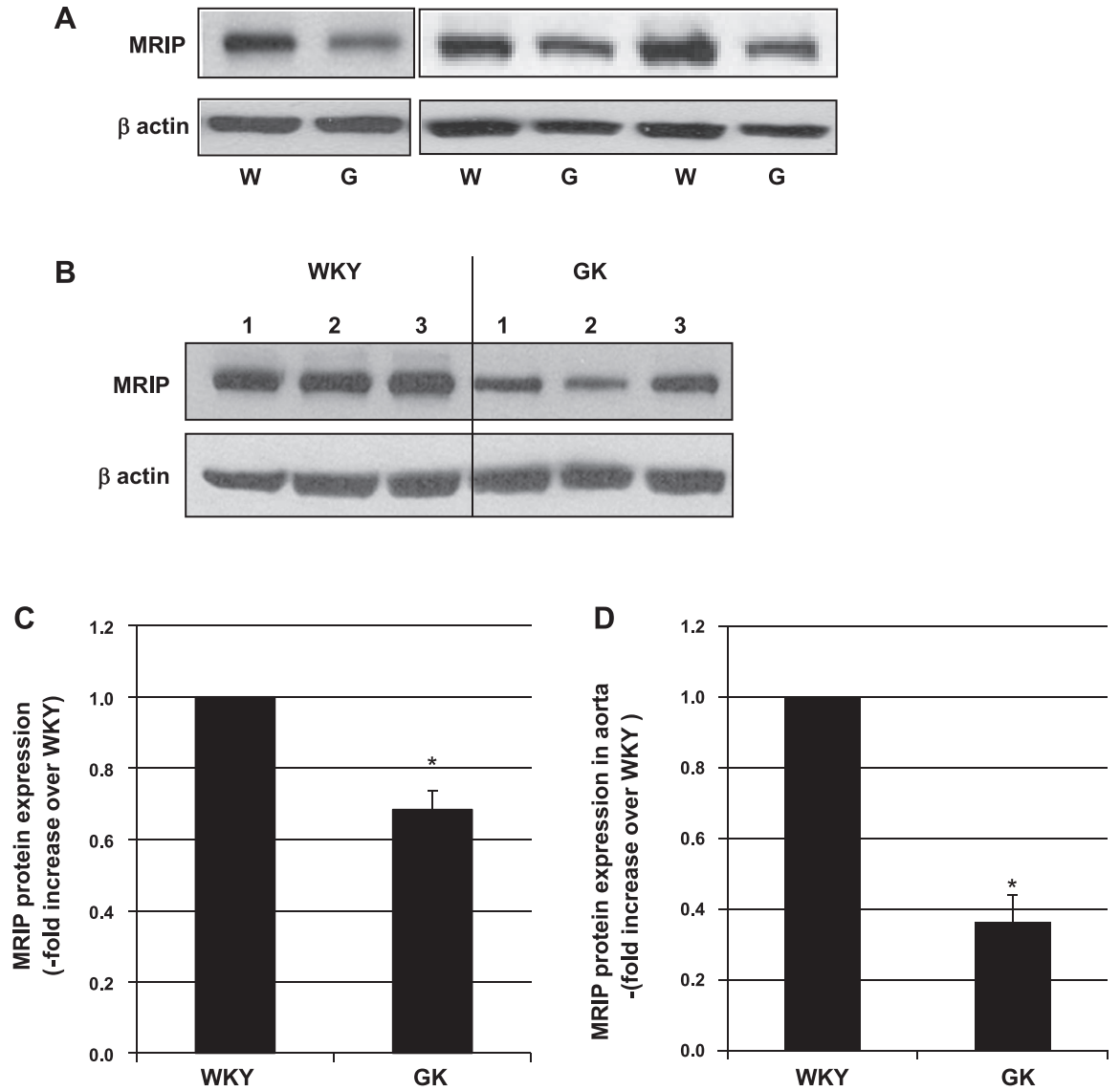

Fig. 2. MRIP expression is lower in Goto-Kakizaki (GK or G) diabetic VSMC and aorta tissue than WKY (W) controls. *A*: VSMCs were cultured for 9–10 days, and equal amounts of protein cell lysates (50 μg) from WKY and GK were isolated and subjected to Western blot analysis as described in MATERIALS AND METHODS. *B*: denuded aorta tissue isolated from either WKY and GK was homogenized to yield protein and subjected to Western blotting. *C*: intensity of MRIP protein expression in WKY and GK VSMCs was quantitated by densitometric analysis and normalized to the abundance of β-actin. $*P < 0.05$ WKY vs. GK; $n = 8$. *D*: intensity of MRIP protein expression in aorta isolated from WKY and GK rats was quantitated by densitometric analysis and normalized to the abundance of β-actin. $*P < 0.05$ WKY vs. GK; $n = 3$.

system (Invitrogen) following the manufacturer's protocol. Immunoprecipitates were heated with sample buffer, containing 2% SDS (Sigma), 0.2 M Tris·HCl (pH 7.5; Bio-Rad), 20 mM EDTA (Sigma), 10% glycerol (Sigma), and bromophenol blue (Sigma) for 10 min at 70°C, and then subjected to SDS-PAGE. The extent of MRIP protein (antibody purchased from Sigma) bound to MYPT1 was normalized to the intensity of total MYPT1 protein.

Western blot analysis. Cells were lysed in a RIPA buffer containing 25 mM Tris·HCl (pH 7.6), 1 mM DTT, 250 mM NaCl, 0.1% SDS, 1% NP-40, and 1% deoxycholate, supplemented with a protease and phosphatase inhibitor cocktail containing 100 mM NaF, 50 mM sodium pyrophosphate, 2 mM sodium orthovanadate, 2 μM microcystin, 50 mM β-glycerophosphate, 1 mM AEBSF, 10 μg/ml leupeptin, and 10 μg/ml aprotinin. Lysates were centrifuged for 30 min at 14,000 *g*. Equal amounts of proteins were heated with sample buffer, containing 2% SDS, 0.2 M Tris·HCl (pH 7.5), 20 mM EDTA, 10% glycerol, and bromophenol blue for 5 min at 95°C, and then loaded on SDS-PAGE. The separated proteins were transferred to nitrocellulose membrane and probed with specific antibodies followed by incubation with horseradish peroxidase-conjugated secondary antibodies (GE Health Care) and detected by enhanced chemiluminescence (ECL; GE Health Care). Proteins were normalized to the intensity of β-actin (Abcam) or total specific protein.

Purification of stress fibers. Purified stress fibers were prepared from WKY and GK VSMCs by glycerol extraction as described (37). Briefly, cells were grown on 100-mm dishes to near confluence, treated with none, 100 nM insulin for 10 or 15 min, ANG II 100 nM for 5 min, or ANG II 100 nM for 5 min followed by insulin 100 nM for 10 min, washed with cold PBS, then extracted with 10 ml of triethanolamine extraction buffer [2.5 mm triethanolamine (Sigma), 1

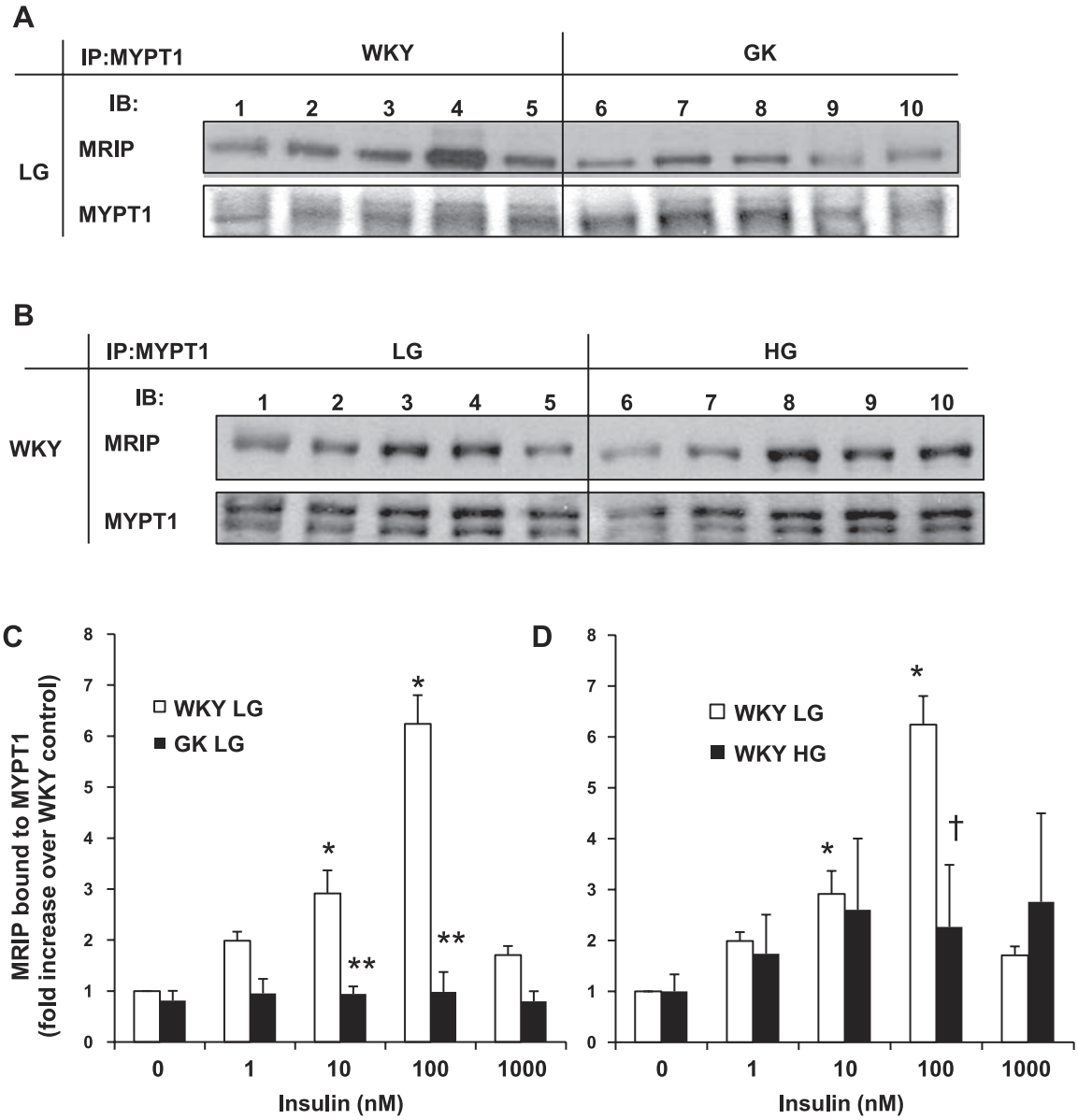

Fig. 3. Insulin increases the binding of MRIP to MYPT1 in a dose-dependent manner in WKY VSMCs and the impaired insulin response in GK diabetic VSMCs. Quiescent VSMCs at *days 9* and *10* were stimulated with insulin [0.0 nM (*lanes 1* and *6*), 1.0 nM (*lanes 2* and *7*), 10 nM (*lanes 3* and *8*), 100 nM (*lanes 4* and *9*) and 1,000 nM (*lanes 5* and *10*)] for 10 min ($n = 7$) in the presence of 20 mM high glucose (HG) or 5 mM glucose (LG). Equal amounts of protein cell lysates (500 μg) were resolved by SDS-PAGE after immunoprecipitation with MYPT1 as described in MATERIALS AND METHODS. *A* and *C*: Western blot analysis of MRIP bound to MYPT1 immunoprecipitates. *C* and *D*: intensity of MRIP protein was quantitated by densitometric analysis and normalized to the abundance of total MYPT1 in WKY comparing LG vs. HG. *$P < 0.05$ control vs. insulin treatment; **$P < 0.05$ WKY vs. GK; †$P < 0.05$ WKY LG vs. HG.

μg/ml leupeptin (Sigma), and pepstatin A (Sigma), 20 μg/ml aprotinin (Sigma)] for 30 min, shaking, with replacement of extraction buffer every 2–3 min. Remaining cell components were then further extracted using 10 ml of glycerol buffer (50% glycerol, 1 μg/ml each of leupeptin and pepstatin A, 20 μg/ml aprotinin in PBS) for 5 min while shaking, with two replacements of extraction buffer. The glycerol was then removed by washing with 10 ml of aprotinin-PBS [20 μg/ml aprotinin, 1 μg/ml of leupeptin and pepstatin A in PBS (Invitrogen)] for 8 min while shaking with one replacement of wash buffer. The remaining insoluble material was scraped in aprotinin-PBS and homogenized with a Z-shaped 21-gauge needle (Becton Dickinson). The insoluble debris was pelleted at 1,000 *g* for 5 min, and stress fibers were isolated by centrifugation of the supernatant at 100,000 *g* for 1 h. The stress fiber pellet was boiled in protein sample buffer and subjected to SDS-PAGE and immunoblotting with the indicated antibodies.

Statistics. The results are presented as means ± SE of four to seven independent experiments. Paired Student's *t*-tests were used to compare the basal versus insulin-treated preparations (see Fig. 2). ANOVA was used to compare the mean values between treatments. $P < 0.05$ was considered statistically significant.

RESULTS

Insulin increases the binding of MRIP to MYPT1 in a time-dependent manner. Previously, our laboratory demonstrated that insulin decreased ANG II-induced MYPT1 phosphorylation on threonine 695 (24). To better understand the role of MRIP on myosin phosphatase in response to insulin, we determined whether MRIP binds to MYPT1 in response to insulin (100 nM). As shown in Fig. 1, *A* and *B*, insulin modulated the binding of MYPT1 to MRIP in a time-dependent manner. In WKY VSMCs, we observed a threefold increase in binding of MYPT1 to MRIP after just 5 min of insulin stimulation (Fig. 1, *A* and *B*). Maximal binding of MRIP to MYPT1 occurred after 30 min whereas 5.5-fold increase over WKY control was observed (Fig. 1, *A* and *B*).

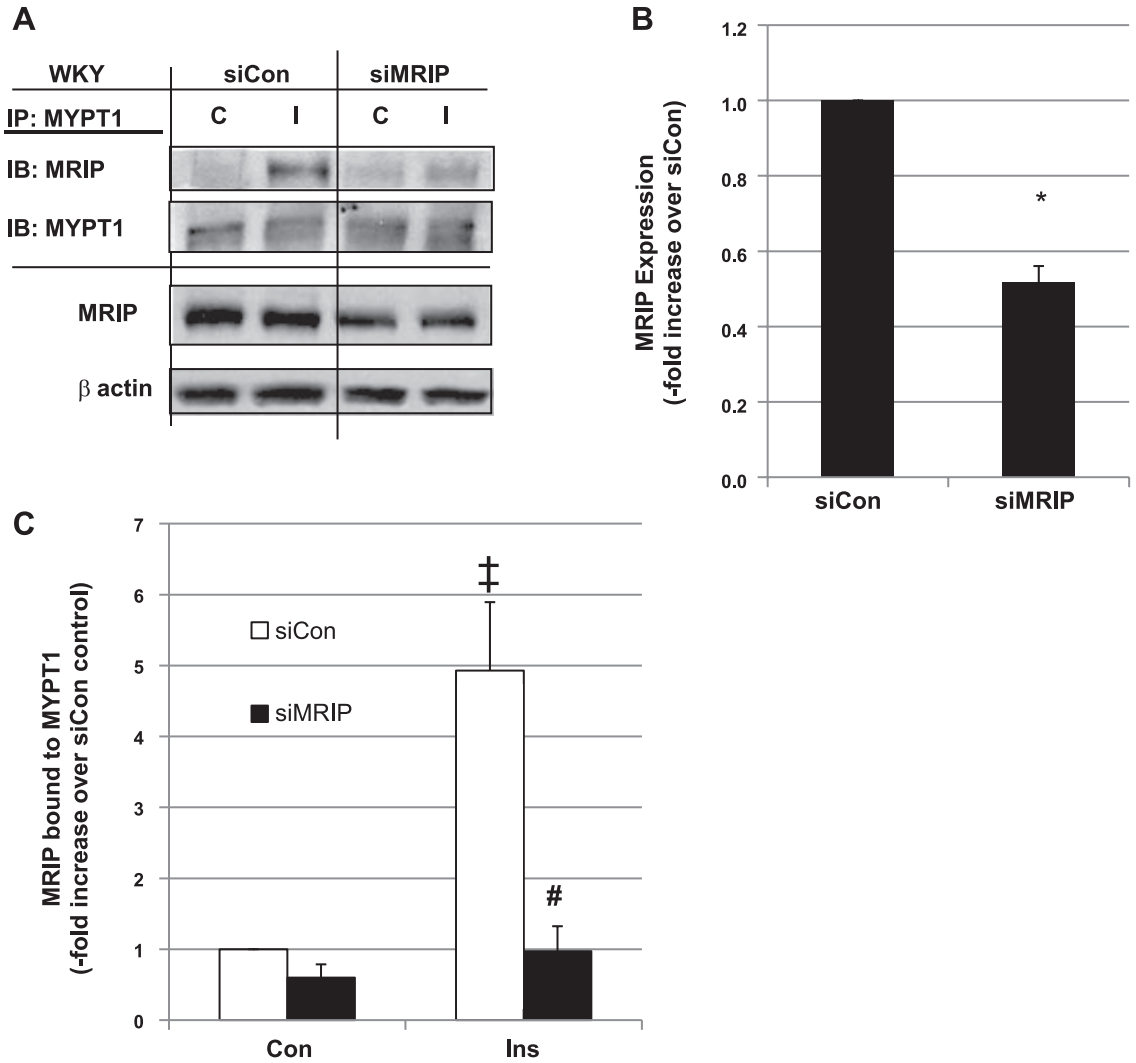

Fig. 4. Impaired insulin-induced MRIP binding to MYPT1 in GK diabetic VSMCs was mimicked by the reduction of MRIP in WKY VSMCs treated with small interfering (si)RNA targeting MRIP. *A*: WKY VSMCs transfected with control siRNA (siCon) or siMRIP for 72 h were serum starved and pulsed with 100 nM insulin for 10 min. Equal amounts of protein cell lysates (500 μg) were resolved by SDS-PAGE after immunoprecipitation with MYPT1 as described in MATERIALS AND METHODS, and the levels of MRIP were quantitated by densitometric analysis and normalized to the abundance of β-actin. *B*: densitometric analyses of MRIP expression after four separate experiments with WKY VSMCs. *$P < 0.05$ siCON vs. siMRIP. *C*: densitometric analyses of MRIP bound to MYPT1 after four separate experiments with WKY VSMCs. ‡$P < 0.05$ control vs. insulin treatment; #$P < 0.05$ siCon vs. siMRIP.

After 60 min, insulin-induced MRIP binding to MYPT1 decreased to a threefold increase over WKY control in WKY VSMCs (Fig. 1, *A* and *B*).

MRIP expression is lower in GK diabetic VSMCs. Next, we compared the expression of MRIP in WKY to diabetic GK VSMCs. MRIP protein expression in GK diabetic VSMCs was 32% less than that of WKY control as determined by Western blotting (Fig. 2, *A* and *C*). We further confirmed the difference in abundance of MRIP protein in aortic tissues isolated from both control WKY and diabetic GK rats. MRIP protein expression in GK diabetic denuded aorta was 63% less than that of WKY control as determined by Western blotting (Fig. 2, *B* and *D*), implying that impaired MRIP expression may play an important role in the impaired insulin-induced diabetic vasodilation observed in diabetes.

Insulin increases the binding of MRIP to MYPT1 in a dose-dependent manner. To better understand the role of MRIP on insulin-induced myosin phosphatase activation, the effect of insulin concentration on the binding of the MRIP to MYPT1 has been assessed. Insulin increased the binding of MYPT1 to MRIP in a dose-dependent manner in VSMCs isolated from WKY rats, as determined by immunoblotting with MRIP after immunoprecipitation with MYPT1 (Fig. 3*A*). Insulin at 1, 10, 100, and 1,000 nM increased the binding of the MYPT1 to MRIP 2.0-, 2.9-, 6.2-, and 1.7-fold over control VSMCs, respectively (Fig. 3*C*; $n = 7$).

Impaired insulin-induced MYPT1 binding to MRIP in GK diabetic VSMC. To determine whether there are any defects in the insulin-stimulated MYPT1 binding to MRIP in diabetes, we tested the binding effect of MYPT1 to MRIP in VSMCs isolated from the GK Type 2 diabetes model. We found that the insulin response to the binding of MRIP to MYPT1 was impaired in GK rats. Insulin at 0, 1, 10, 100, and 1,000 nM only induced the MYPT1 binding to MRIP by 0.8-, 1.0-, 1.0-, 1.0-, and 0.8-fold over the WKY control, respectively (Fig. 3, *A* and *C*; $n = 6$). Insulin resistance in diabetes may be the result of the high glucose (HG) stimulation. To determine whether HG modulates insulin-stimulated binding of MRIP to MYPT1 any differently, we stimulated WKY cells with HG (20 mM). The binding of MRIP to MYPT1 in response to 0, 1, 10, 100, and 1,000 nM insulin were 1-, 1.7-, 2.6-, 2.3-, and 2.8-fold over the WKY HG control. The binding of MYPT1 to MRIP in response to 100 nM was reduced by 66% in WKY VSMCs cultured in HG to mimic the diabetic VSMC environment, when compared with that of WKY VSMCs treated in 5 mM glucose (Fig. 3, *B* and *D*).

Reduction of MRIP in WKY VSMCs by treatment with siRNA targeting MRIP impairs insulin-induced MRIP binding to MYPT1 and mimics GK diabetic VSMCs. To confirm the impaired binding of MRIP to MYPT1 in response to insulin in GK diabetic VSMC, siRNA targeting MRIP (siMRIP) was generated to reduce the MRIP protein expression in WKY VSMCs to mimic the level of MRIP expression in GK diabetic VSMCs. siMRIP reduced the MRIP amount in WKY VSMCs by 44% (Fig. 4, *A* and *B*). As shown in Fig. 4, *A* and *C*, insulin induced the binding of MYPT1 to MRIP in control siRNA (siCon)-treated WKY VSMCs to fivefold over controls (Fig. 4*A*; *lanes 1* and *2*), while in siMRIP-treated WKY VSMCs, insulin failed to induce the binding of MYPT1 to MRIP in response to insulin (Fig. 4*A, lanes 3* and *4,* and Fig. 4*C*).

ANG II pretreatment inhibits insulin-induced MRIP binding to MYPT1. Previously, our laboratory demonstrated that the insulin-induced vasodilation in VSMCs was inhibited by the contractile agent, ANG II (25, 26). Pretreatment of cells with ANG II (100 nM) for 5 min prior to insulin treatment for 10 min or vice versa (Fig. 5, *A* and *B*; *lanes 4* and *5*) inhibited the MRIP binding to MYPT1 by 74% compared with that of insulin by itself in WKY VSMCs (Fig. 5*A*, *lane 3*, and Fig. 5*B*). In GK VSMCs, the inhibitory action of ANG II on insulin-induced MRIP to MYPT1 binding was not obvious because of the insignificant insulin-induced MRIP-MYPT1 binding (Fig. 5*A*).

Insulin induces MRIP translocation out of stress fiber in WKY, while GK VSMCs appear insulin resistant. The stress fiber is the place where myosin phosphorylation occurs when contractile agents stimulate the phosphorylation of MYPT1. The presence of MRIP in stress fibers is required to exert a contractile signal which causes the phosphorylation of myosin (37). In contrast, insulin, a potent relaxation agent, may cause the translocation of MRIP out of the stress fiber. To test this, we isolated stress fibers from WKY and GK cells treated with either PBS or insulin. As shown in Fig. 6*A*, insulin induced nearly 60% of MRIP to translocate out of F-actin in WKY rats,

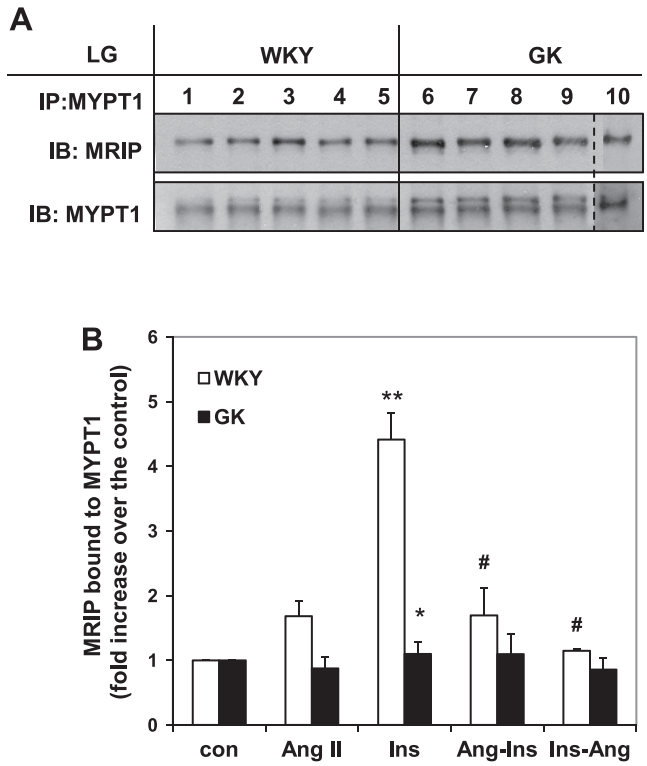

Fig. 5. Angiotensin II (ANG II) pretreatment inhibits the insulin-induced MRIP binding to MYPT1. Quiescent VSMCs at *day 9* were stimulated with ANG II (100 nM) for 10 min, insulin (100 nM) for 10 min, ANG II (100 nM) for 5 min followed by insulin (100 nM) for 10 min, and insulin (100 nM) followed by ANG II (100 nM) for 5 min. Equal amounts of protein cell lysates (500 μg) were resolved by SDS-PAGE after immunoprecipitation with MYPT1 as described in MATERIALS AND METHODS. *A*: MRIP and MYPT1 were measured by Western blot analysis. *Lane 10* was prepared on a different membrane but exposed on the same film for presentation. *B*: MRIP intensity was quantitated by densitometric analysis and normalized to the abundance of introduced MYPT1. *$P < 0.05$ WKY vs. GK; **$P < 0.05$ control vs. insulin; #$P < 0.05$ insulin vs. ANG II-Ins or Ins-ANG II; $n = 3$.

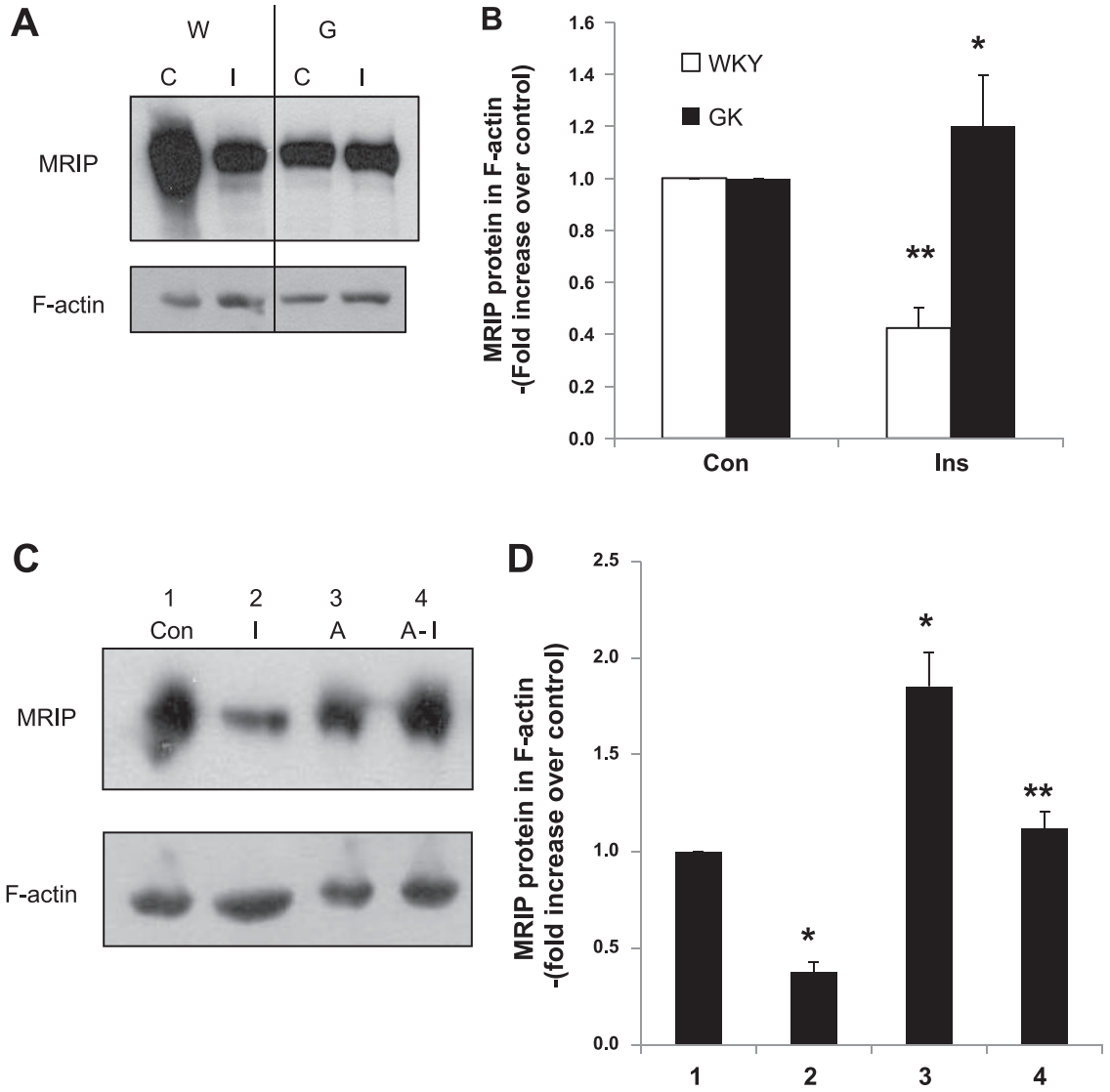

Fig. 6. Insulin induces the translocation of MRIP out of stress fiber in WKY VSMCs, while GK VSMCs show insulin resistance on MRIP translocation. Quiescent VSMCs at *day 9* were stimulated with insulin (100 nM) for 10 min. *A*: stress fibers isolated from cells after exposure were dissolved in sample loading buffer, resolved by SDS-PAGE, and transferred to nitrocellulose membrane. The levels of MRIP protein in the stress fiber were measured by Western blot analysis. Lanes were removed to present relevant data. MRIP intensity was quantitated by densitometric analysis and normalized to the abundance of introduced F-actin. C, control; I, insulin. *B*: densitometric measurements. Insulin induces MRIP out of stress fiber in WKY, while ANG II causes the translocation of MRIP to stress fiber. $*P < 0.05$ WKY vs. GK; $**P < 0.05$ control vs. insulin; $n = 3$. *C*: stress fibers isolated from cells after exposure were dissolved in sample loading buffer, resolved by SDS-PAGE, and transferred to nitrocellulose membrane. The levels of MRIP protein in the stress fiber were measured by Western blot analysis. MRIP intensity was quantitated by densitometric analysis and normalized to the abundance of introduced F-actin. *D*: densitometric measurements. $*P < 0.05$ control vs. insulin (I) or ANG II (A); $**P < 0.05$ A vs. ANG II-Ins (A-I); $n = 3$.

while in GK rats, insulin failed to translocate MRIP (Fig. 6, *A* and *B*).

Insulin induces MRIP out of stress fiber in WKY rats, while ANG II causes the translocation of MRIP to stress fiber. We previously showed that ANG II phosphorylates MYPT1 and that insulin antagonizes this by dephosphorylation of MYPT1 (7). We tested whether the vasorelaxant insulin and the vasoconstrictor ANG II caused the MRIP translocation from stress fiber, differently. Insulin induces MRIP translocation out of stress fiber in WKY rats, while ANG II causes the translocation of MRIP to stress fiber. As the presence of MRIP in stress fiber is required for phosphorylation of myosin (14), the vasocontractile ANG II, which is known to phosphorylate myosin, causes the translocation of MRIP into the stress fiber, while the vasorelaxant insulin reduces the amount of MRIP in stress fiber. ANG II induces the increase of MRIP protein content in stress fiber twofold compared with that of the control (Fig. 6, *C* and *D*).

MRIP adenovirus overexpression restores impaired GK MRIP binding to MYPT1. Since reduced MRIP expression seemed to cause impaired insulin-induced MRIP binding to MYPT1 in GK VSMCs, we created an MRIP adenovirus construct, Ad-MRIP-FLAG (Ad-MRIP), to overexpress MRIP in GK VSMCs. We then determined whether the increased MRIP expression could restore the insulin-induced MRIP binding to MYPT1 in GK diabetic VSMCs. Ad-MRIP induced a twofold overexpression of MRIP in GK VSMCs over Ad5CMV control (Ad-Con), to mimic the level of WKY MRIP protein

contents based on the finding in Fig. 2 (Fig. 7*A*, third panel, *lanes 1* and *2* vs. *lanes 3* and *4*; Fig. 7*B*). Basal MRIP binding to MYPT1 was increased threefold by Ad-MRIP in GK VSMCs over Ad-CON (Fig. 7*A*, *lane 1* vs. *lane 3*, and Fig. 7*C*). Insulin increased MRIP binding to MYPT1 in GK VSMCs overexpressing MRIP to 4.3-fold over control of Ad-Con (Fig. 7*A*, *lane 1* vs. *lane 4*; and Fig. 7*C*).

DISCUSSION

This is the first study to demonstrate that insulin stimulates the binding of MRIP to MYPT1. In addition, we demonstrate impaired MRIP expression in GK diabetic VSMCs as well as insulin-resistant MRIP to MYPT1 binding. Gene silencing of MRIP in WKY VSMCs, using siRNA, mimics the impaired MRIP to MYPT1 binding observed in GK VSMCs. Moreover, overexpression of MRIP in GK diabetic VSMCs reestablished insulin-stimulated MRIP to MYPT1 binding, suggesting that the impaired insulin-induced vasodilation in diabetes may be due, in part, to the absence of MRIP to MYPT1 binding and its subsequent effect on MLCP.

Insulin-induced binding of MRIP to MYPT1 plays an important role in relaying the vasodilatory signal to dephosphorylate the myosin light chain contractile filament, which may proceed via cGK1α activation. Previously, our laboratory dem-

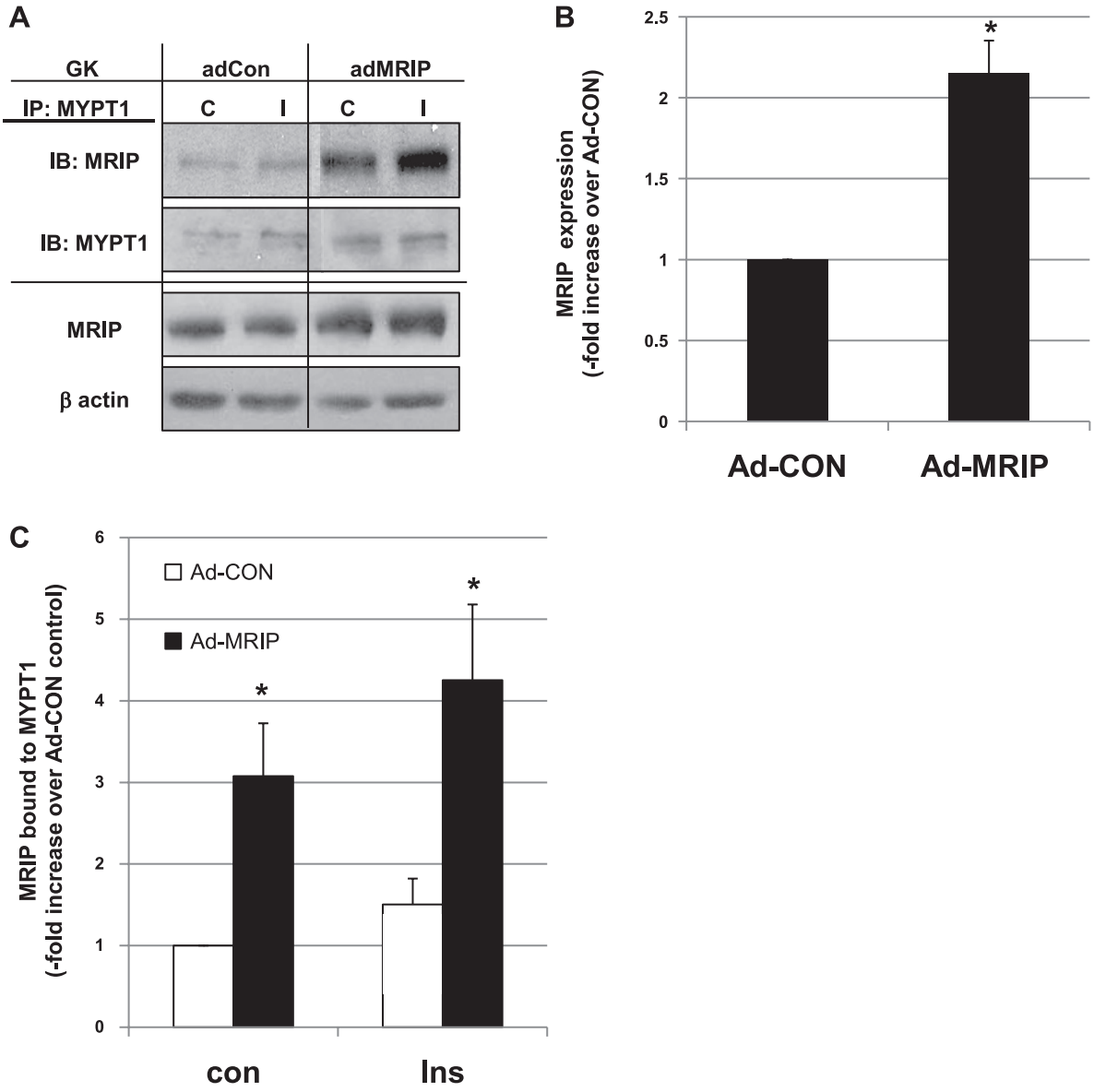

Fig. 7. Overexpression of MRIP restores insulin-induced MRIP binding to MYPT1 in GK VSMCs. VSMCs at 80% confluence were washed with serum-free media and treated with adenovirus (Ad)-CMV (Ad-CON) or Ad-MRIP-FLAG (Ad-MRIP) for 4 h, then treated with serum and incubated overnight. The next day, cells were washed with fresh media and cultured for an additional 24 h. Serum-starved cells (24 h) were exposed to 100 nM insulin for 10 min where indicated. Equal amounts of protein cell lysates (500 μg) were either solubilized with sample loading buffer or resolved by SDS-PAGE after immunoprecipitation with MYPT1 as described in MATERIALS AND METHODS. *A*: the levels of total MRIP and β-actin, and MYPT1 immunoprecipitated MRIP and total MYPT1 were measured by Western blot analysis. The blots for the IP experiments were all on the same membrane and aligned to follow the order of treatment. *B*: densitometric analyses of MRIP expression after three separate experiments with GK VSMCs. *C*: densitometric analyses of MRIP bound to MYPT1 after three separate experiments with GK VSMCs. *$P < 0.05$ Ad-CON vs. Ad-MRIP; $n = 3$.

onstrated that the insulin is a potent vasodilator of VSMCs through IRS-1→PI3-K→iNOS→NO-cGMP and cGK1α signaling; insulin inhibits RhoA/ROK activity by inducing an accumulation of cGMP and activating cGKIα (5). The exact mechanism by which RhoA signals stress fiber contraction, however, remains unknown. We assume that the combination of RhoA binding to MRIP and subsequent cGK1α activation may exert the signal. Surks et al. (36) demonstrated that MYPT1 can bind MRIP and cGK1α simultaneously since MRIP can interact with cGK1α as demonstrated by coimmunoprecipitation. Even though the binding between MRIP and cGK1α are not direct and possibly involve the intermediary action of MYPT1, we speculate that insulin-induced cGK1α activation may also trigger the binding of MRIP to MYPT1, to facilitate MLCP activation. We believe that insulin-induced cGMP/cGK1α inhibits RhoA/Rho-kinase activation, and thereby cGK1α and MYPT1 interaction with MRIP causes MYPT1 dephosphorylation and MLCP activation. Consequently, MLCP will dephosphorylate MLC20 and lead to VSMC vasodilation. Future studies will be needed to clarify the binding of cGK1α to MYPT1 and the MRIP complex in response to insulin stimulation.

One role of MRIP is to regulate the contractile state of VSM by controlling MLCP (11, 34). The location of MRIP is known to be within the contractile filament where MLC20 phosphorylation regulates the contractile state (36). Surks et al. (37) have shown that MRIP colocalizes with actin-myosin stress fibers, and others have found that MRIP can bind both actin and myosin (27, 37), suggesting a role for MRIP in targeting of the MLCP complex. We believe that translocation of MRIP out of contractile filaments may effectively control MLCP in rat VSMCs. Using glycerol-extracted stress fibers to detect the MRIP (36), we demonstrated that 10 min of insulin stimulation caused MRIP translocation out of F-actin (Fig. 6). While MRIP localized with F-actin, as determined by fluorescence immunohistochemistry, p116RIP3, the murine form of MRIP, has also been found in the cell nucleus (12). This finding correlates well with our current observations. Since we used rat VSMCs for the current study, translocated MRIP may have been translocated to the cytosol, perinuclear region, or even in the nucleus, upon insulin stimulation. Further studies are needed to investigate the exact organelles responsible for the vasodilatory response of MRIP.

We attribute the impaired insulin-induced binding of MRIP to MYPT1 in diabetic VSMCs to the lower levels of MRIP protein observed in the GK diabetic VSMCs versus protein modification for two reasons. First, reducing MRIP protein levels in control WKY VSMCs using siRNA targeting MRIP mimics the diabetic GK insulin response (Fig. 4), and second, there is an increase in the amount of MRIP bound to MYPT1 with overexpression of MRIP in GK VSMCs (Fig. 7).

The binding of RhoA to MRIP may facilitate vasodilation as well as contractile signaling. Both inactive and active forms of RhoA may bind to MRIP via the presentation of GDP or GTP, respectively. Depending on the activity of RhoA, MRIP may act as the chaperone to send either contractile or vasodilatory signals to MYPT1. This hypothesis is based on the finding that both inactive GDPβS and active GTPγS are found to be bound to MRIP (36). Insulin, which inhibits RhoA activation, may induce GDPβS binding to MRIP. Therefore, we have hypothesized that insulin inhibits the phosphorylation of MYPT1 at Thr696 by accommodating the interaction of inactive RhoA-MRIP-MYPT1, resulting in relaxation of VSM. We introduce the possibility that insulin inhibition of RhoA activity results in the interaction of MRIP, and thereby controls MLCP activity. Furthermore, it has been shown that amino acids 545–878 of MRIP, via adjacent RhoA- and MYPT1-binding domains, mediate binding of both RhoA and MYPT1 (36). Activated RhoA and Rho kinase translocate to the cell membrane, and a subpopulation of RhoA/ROK has been identified on the actin stress fiber (7). Future investigation is needed to examine the regulation of MLCP by insulin via RhoA-MRIP interaction.

Hypertension and diabetes are accompanied by upregulation of Rho kinase activity, resulting in an increase in ROK-α/

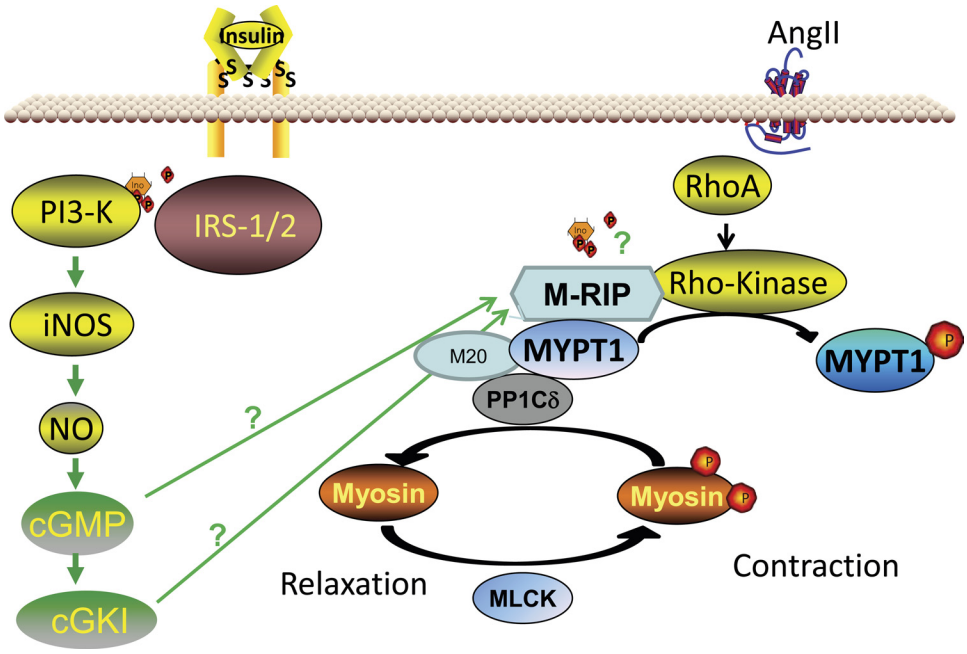

Fig. 8. Schematic representation of the insulin-induced MRIP binding to MYPT1. Contractile agonists such as ANG II lead to activation of RhoA. Activated RhoA binds to and activates Rho kinase, leading to MYPT1 phosphorylation and inhibition of myosin light chain kinase (MLCK) and phosphatase (MLCP), resulting in vessel contraction. Insulin-induced insulin receptor substrate-1 (IRS-1) tyrosine phosphorylation activates phosphatidylinositol 3-kinase (PI3-K)/Akt and the expression of inducible nitric oxide synthase (iNOS). Insulin's vasodilatory effects are mediated by NO produced by iNOS, which then activates cyclic guanosine-3′,5′-monophosphate (cGMP)-dependent protein kinase 1α (cGKIα) and results in the dephosphorylation of threonine 696 on a MYPT1 and the subsequent inactivation of RhoA and Rho-associated kinase-α (ROK-α). MRIP binds to MYPT1 upon insulin stimulation, which regulates vasodilation, most likely by a reduction of MLC20 (M20) phosphorylation, which results in the vasodilation of SMC.

IRS-1 association, inhibition of insulin signaling upstream of PI3-K, iNOS induction, NO/cGMP generation, and MLCP activation (6). Our previous data indicate that in the nonobese Type 2 diabetes GK model, rat aortic RhoA/Rho-kinase activity is increased when compared with that of the control as determined by isometric tension measurement (26). Because Rho-kinase is upstream of MYPT1, the increased phosphorylation of MYPT1 parallels Rho-kinase activity (10, 19). In this model, insulin signaling is also impaired; insulin-induced tyrosine phosphorylation of IRS-1 is reduced along with PI3-K and AKT activities, resulting in decreased MLCP activity (32). Therefore, we hypothesize that impaired insulin-induced RhoA inhibition along with increased RhoA activity in GK aorta and VSMCs (10, 19) may result in the abnormal expression and regulation of MRIP. We demonstrate here that insulin's control of RhoA-MRIP regulation of MLCP was impaired in GK VSMCs (Fig. 8), which correlates well with our previous findings in which Rho kinase activity was increased in GK VSMCs (24, 26).

The current study demonstrates that MRIP is an insulin-responsive regulatory and trafficking protein of MLCP via its binding to MYPT1. Moreover, insulin induces the translocation of MRIP out of stress fibers. In our GK model of Type 2 diabetes we observe diminished MRIP expression, failure of insulin to induce the binding of MRIP to MYPT1 as well as the translocation of MRIP out of stress fibers. These data may partially explain the impaired vasodilatory signal in response to insulin and the exaggerated contractile status in the diabetic vasculature.

ACKNOWLEDGMENTS

The authors thank the University of Iowa, Gene Transfer Vector Core for preparation of the adenovirus constructed with MRIP-FLAG.

GRANTS

This study was supported in part by American Diabetes Association Grant 1-10-BS-147.

DISCLOSURES

No conflicts of interest, financial or otherwise, are declared by J. H. Lee and T. Palaia. L. Ragolia has a service contract agreement with Reata Pharmaceuticals.

AUTHOR CONTRIBUTIONS

J.H.L. and L.R. conception and design of the research; J.H.L., T.P., and L.R. performed the experiments; J.H.L., T.P., and L.R. analyzed the data; J.H.L. and L.R. interpreted the results of the experiments; J.H.L. and L.R. prepared the figures; J.H.L. and L.R. drafted the manuscript; L.R. edited and revised the manuscript; L.R. approved the final version of the manuscript.

REFERENCES

1. **Anderson RD, Haskell RE, Xia H, Roessler BJ, Davidson L.** A simple method for the rapid generation of recombinant adenovirus vectors. *Gene Ther* 7: 1034–1038, 2000.
2. **Begum N, Duddy N, Sandu O, Reinzie J, Ragolia L.** Regulation of myosin-bound protein phosphatase by insulin in vascular smooth muscle cells: evaluation of the role of Rho kinase and phosphatidylinositol-3-kinase-dependent signaling pathways. *Mol Endocrinol* 14: 1365–1376, 2000.
3. **Begum N, Ragolia L.** Altered regulation of insulin signaling components in adipocytes of insulin-resistant type II diabetic Goto-Kakizaki rats. *Metabolism* 47: 54–62, 1998.
4. **Begum N, Ragolia L, Rienzie J, McCarthy M, Duddy N.** Regulation of mitogen-activated protein kinase phosphatase-1 induction by insulin in vascular smooth muscle cells. Evaluation of the role of the nitric oxide signaling pathway and potential defects in hypertension. *J Biol Chem* 273: 25164–25170, 1998.
5. **Begum N, Sandu OA, Duddy N.** Negative regulation of Rho signaling by insulin and its impact on actin cytoskeleton organization in vascular smooth muscle cells: role of nitric oxide and cyclic guanosine monophosphate signaling pathways. *Diabetes* 51: 2256–2263, 2002.
6. **Begum N, Sandu OA, Ito M, Lohmann SM, Smolenski A.** Active Rho kinase (ROK-alpha) associates with insulin receptor substrate-1 and inhibits insulin signaling in vascular smooth muscle cells. *J Biol Chem* 277: 6214–6222, 2002.
7. **Chen XQ, Tan I, Ng CH, Hall C, Lim L, Leung T.** Characterization of RhoA-binding kinase ROKα implication of the pleckstrin homology domain in ROKα function using region-specific antibodies. *J Biol Chem* 277: 12680–12688, 2002.
8. **Colwell J, Jokl R.** *Diabetes Mellitus: Theory and Practice*. Norwalk, CT: Appleton and Lange, 1996.
9. **Eto M, Senba S, Morita F, Yazawa M.** Molecular cloning of a novel phosphorylation-dependent inhibitory protein of protein phosphatase-1 (CPI17) in smooth muscle: its specific localization in smooth muscle. *FEBS Lett* 410: 356–360, 1997.
10. **Feng J, Ito M, Ichikawa K, Isaka N, Nishikawa M, Hartshorne DJ, Nakano T.** Inhibitory phosphorylation site for Rho-associated kinase on smooth muscle myosin phosphatase. *J Biol Chem* 274: 37385–37390, 1999.
11. **Fukata Y, Amano M, Kaibuchi K.** Rho-Rho-kinase pathway in smooth muscle contraction and cytoskeletal reorganization of non-muscle cells. *Trends Pharmacol Sci* 22: 32–39, 2001.
12. **Gebbink MF, Kranenburg O, Poland M, van Horck FP, Houssa B, Moolenaar WH.** Identification of a novel, putative Rho-specific GDP/GTP exchange factor and a RhoA-binding protein: control of neuronal morphology. *J Cell Biol* 137: 1603–1613, 1997.
13. **Gong M, Fuglsang A, Alessi D, Kobayashi S, Cohen P, Somlyo A, Somlyo A.** Arachidonic acid inhibits myosin light chain phosphatase and sensitizes smooth muscle to calcium. *J Biol Chem* 267: 21492–21498, 1992.
14. **Hartshorne D, Ito M, Erdödi F.** Myosin light chain phosphatase: subunit composition, interactions and regulation. *J Muscle Res Cell Motil* 19: 325–341, 1998.
15. **Hsueh W, Law R.** Insulin signaling in the arterial wall. *Am J Cardiol* 84: 21J–24J, 1999.
16. **Ichikawa K, Ito M, Hartshorne DJ.** Phosphorylation of the large subunit of myosin phosphatase and inhibition of phosphatase activity. *J Biol Chem* 271: 4733–4740, 1996.
17. **Kahn AM, Allen JC, Seidel CL, Zhang S.** Insulin inhibits migration of vascular smooth muscle cells with inducible nitric oxide synthase. *Hypertension* 35: 303–306, 2000.
18. **Kahn AM, Husid A, Allen JC, Seidel CL, Song T.** Insulin acutely inhibits cultured vascular smooth muscle cell contraction by a nitric oxide synthase-dependent pathway. *Hypertension* 30: 928–933, 1997.
19. **Kimura K, Ito M, Amano M, Chihara K, Fukata Y, Nakafuku M, Yamamori B, Feng J, Nakano T, Okawa K, Iwamatsu A, Kaibuchi K.** Regulation of myosin phosphatase by Rho and Rho-associated kinase (Rho-kinase). *Science* 273: 245–248, 1996.
20. **Kitazawa T, Eto M, Woodsome TP, Brautigan DL.** Agonists trigger G protein-mediated activation of the CPI-17 inhibitor phosphoprotein of myosin light chain phosphatase to enhance vascular smooth muscle contractility. *J Biol Chem* 275: 9897–9900, 2000.
21. **Kitazawa T, Takizawa N, Ikebe M, Eto M.** Reconstitution of protein kinase C-induced contractile Ca^{2+} sensitization in Triton X-100-demembranated rabbit arterial smooth muscle. *J Physiol* 520: 139–152, 1999.
22. **Koga Y, Ikebe M.** p116Rip decreases myosin II phosphorylation by activating myosin light chain phosphatase and by inactivating RhoA. *J Biol Chem* 280: 4983–4991, 2005.
23. **Kureishi Y, Kobayashi S, Amano M, Kimura K, Kanaide H, Nakano T, Kaibuchi K, Ito M.** Rho-associated kinase directly induces smooth muscle contraction through myosin light chain phosphorylation. *J Biol Chem* 272: 12257–12260, 1997.
24. **Lee JH, Palaia T, Ragolia L.** Impaired insulin-mediated vasorelaxation in diabetic Goto-Kakizaki rats is caused by impaired Akt phosphorylation. *Am J Physiol Cell Physiol* 296: C327–C338, 2009.
25. **Lee JH, Ragolia L.** AKT phosphorylation is essential for insulin-induced relaxation of rat vascular smooth muscle cells. *Am J Physiol Cell Physiol* 291: C1355–C1365, 2006.

26. **Lee JH, Xia S, Ragolia L.** Upregulation of AT2 receptor and iNOS impairs angiotensin II-induced contraction without endothelium influence in young normotensive diabetic rats. *Am J Physiol Regul Integr Comp Physiol* 295: R144–R154, 2008.
27. **Mulder J, Poland M, Gebbink MF, Calafat J, Moolenaar WH, Kranenburg O.** p116Rip is a novel filamentous actin-binding protein. *J Biol Chem* 278: 27216–27223, 2003.
28. **Okon E, Szado T, Laher I, McManus B, van Breemen C.** Augmented contractile response of vascular smooth muscle in a diabetic mouse model. *J Vasc Res* 40: 520–530, 2003.
29. **Okubo S, Ito M, Takashiba Y, Ichikawa K, Miyahara M, Shimizu H, Konishi T, Shima H, Nagao M, Hartshorne D, Nakano T.** A regulatory subunit of smooth muscle myosin bound phosphatase. *Biochem Biophys Res Commun* 200: 429–434, 1994.
30. **Riddick N, Ohtani K, Surks H.** Targeting by myosin phosphatase-RhoA interacting protein mediates RhoA/ROCK regulation of myosin phosphatase. *J Cell Biochem* 103: 1158–1170, 2008.
32. **Sandu O, Ragolia L, Begum N.** Diabetes in the Goto-Kakizaki rat is accompanied by impaired insulin-mediated myosin-bound phosphatase activation and vascular smooth muscle cell relaxation. *Diabetes* 49: 2178–2189, 2000.
33. **Seko T, Ito M, Kureishi Y, Okamoto R, Moriki N, Onishi K, Isaka N, Hartshorne DJ, Nakano T.** Activation of RhoA and inhibition of myosin phosphatase as important components in hypertension in vascular smooth muscle. *Circ Res* 92: 411–418, 2003.
34. **Somlyo A, Somlyo A.** Signal transduction and regulation in smooth muscle. *Nature* 372: 231–236, 1994.
35. **Sowers JR, Epstein M, Frohlich ED.** Diabetes, hypertension, and cardiovascular disease: an update. *Hypertension* 37: 1053–1059, 2001.
36. **Surks HK, Richards CT, Mendelsohn ME.** Myosin phosphatase-Rho interacting protein: a new member of the myosin phosphatase Complex That Directly Binds RhoA. *J Biol Chem* 278: 51484–51493, 2003.
37. **Surks HK, Riddick N, Ohtani K.** M-RIP targets myosin phosphatase to stress fibers to regulate myosin light chain phosphorylation in vascular smooth muscle cells. *J Biol Chem* 280: 42543–42551, 2005.
38. **Sward K, Mita M, Wilson D, Deng J, Susnjar M, Walsh M.** The role of RhoA and Rho-associated kinase in vascular smooth muscle contraction. *Curr Hypertens Rep* 5: 66–72, 2003.
39. **Trinkle-Mulcahy L, Ichikawa K, Hartshorne DJ, Siegman MJ, Butler TM.** Thiophosphorylation of the 130-kDa subunit is associated with a decreased activity of myosin light chain phosphatase in alpha-toxin-permeabilized smooth muscle. *J Biol Chem* 270: 18191–18194, 1995.